Functional Ecology

# Climate and soil microorganisms drive soil phosphorus fractions in coastal dune systems

Laura García-Velázquez[1], Alexandra Rodríguez[2], Antonio Gallardo[1], Fernando T. Maestre[3,4], Everaldo Dos Santos[5], Angela Lafuente[6], María José Fernández-Alonso[2], Brajesh K. Singh[7,8], Jun-Tao Wang[7,8] & Jorge Durán[2]

**Correspondence**: Laura García-Velázquez

Email: garciavelazquezlaura@gmail.com

[1]Departamento de Sistemas Físicos, Químicos y Naturales, Universidad Pablo de Olavide, Crta. Utrera Km 1, 41013 Sevilla, Spain

[2]Centre for Functional Ecology (CFE) - Science for People & the Planet, University of Coimbra, Calçada Martim de Freitas, 3000-456 Coimbra, Portugal

[3]Departamento de Ecología, Universidad de Alicante, Carretera de San Vicente del Raspeig s/n, 03690 San Vicente del Raspeig, Alicante, Spain

[4]Instituto Multidisciplinar para el Estudio del Medio "Ramón Margalef", Universidad de Alicante, Carretera de San Vicente del Raspeig s/n, 03690 San Vicente del Raspeig, Alicante, Spain

[5]Eixo de recursos naturais/meio ambiente, Campus Paranaguá-PR, Instituto Federal do Paraná, CEP 83215-750 Nº 453, Paranaguá, Brazil

[6]Departamento de Biología y Geología, Física y Química Inorgánica, Escuela Superior de Ciencias Experimentales y Tecnología, Universidad Rey Juan Carlos, Calle Tulipán s/n, 28933 Móstoles, Spain

[7]Hawkesbury Institute for the Environment, Western Sydney University, Penrith, NSW 2751, Australia

[8]Global Centre for Land-Based Innovation, Western Sydney University, Penrith, NSW 2751, Australia

This article has been accepted for publication and undergone full peer review but has not been through the copyediting, typesetting, pagination and proofreading process, which may lead to differences between this version and the Version of Record. Please cite this article as doi: 10.1111/1365-2435.13606

**Acknowledgments**

We thank to Diego Soler who assisted with laboratory work and Jesús Rodríguez for unconditional support in difficult times and his valuable logistic help during the sampling. This project was financed by FEDER/Ministerio de Ciencia, Innovación y Universidades- Agencia Estatal de Investigación/Proyect (CGL2017-88124-R), European Research Council (ERC Grant Agreement 647038 [BIODESERT]) and the Fundação para Ciência e Tecnologia (IF/00950/2014) and the FEDER, within the PT2020 Partnership Agreement and COMPETE 2020 (UID/BIA/04004/2013). FTM acknowledges support from Generalitat Valenciana (CIDEGENT/2018/041). BKS acknowledge research support on microbes and ecosystem functions from the Australian Research Council (DP170104634) and Research Award from the Humboldt Foundation. The authors declare no competing financial interests.

**Authors' contribution**

AR, AG, FTM and JD conceived the study and designed methodology. LGV, AR, EDS and JD collected the data. LGV, AR, AL, MJFA, JTW, BKS and JD analysed the data. LGV led the writing of the manuscript. All authors contributed critically to the drafts and gave final approval for publication.

**Data availability**

The data used in the primary analyses are available upon request and without any restriction, and are published in figshare: 10.6084/m9.figshare.11309615 (García-Velázquez et al., 2019).

MS LAURA GARCÍA-VELÁZQUEZ (Orcid ID : 0000-0003-3290-7531)

MS ANGELA LAFUENTE (Orcid ID : 0000-0001-9626-0373)

PROFESSOR BRAJESH SINGH (Orcid ID : 0000-0003-4413-4185)

DR JORGE DURÁN (Orcid ID : 0000-0002-7375-5290)

Article type : Research Article

Editor : Faming Wang

Section : Ecosystems Ecology

**Abstract**

1. The importance of soil phosphorus (P) is likely to increase in coming decades due to the growing atmospheric nitrogen (N) deposition originated by industrial and agricultural activities. We currently lack a proper understanding of the main drivers of soil P pools in coastal dunes, which rank among the most valued priority conservation areas worldwide.
2. Here we evaluated the joint effects of biotic (i.e. microbial abundance and richness, vegetation and cryptogams cover) and abiotic (i.e. pH and aridity) factors on labile, medium-lability and recalcitrant soil P pools across a wide aridity gradient in the Atlantic coast of the Iberian Peninsula.
3. Climate determined the availability of medium-lability, recalcitrant and total P, but had a minor net effect on labile P, which was positively and significantly related to the presence of plants, mosses and lichens. Medium-lability P was significantly influenced by soil bacterial richness and abundance (positively and negatively, respectively).
4. Our results suggest that microorganisms transfer P from medium-lability pool to more labile one. At the same time, increases in bacterial richness associated to biofilms

might be involved in the thickening of the medium-lability P pool in our climosequence.

5. These bacterial-mediated transfers would confer resistance to the labile P pool under future climate change and uncover an important role of soil microorganisms as modulators of the geochemical P cycle.

**Keywords**: biofilms, climosequence, coastal dunes, global change, medium-lability phosphorus, microbial transfer model, phosphorus pools

**Resumen**

1. Es probable que la importancia del fósforo (P) del suelo aumente en las próximas décadas debido a la creciente deposición atmosférica de nitrógeno (N) originada por las actividades agrícolas e industriales. Actualmente no tenemos un conocimiento adecuado de los principales factores que controlan las fracciones de P del suelo en dunas costeras, las cuales se encuentran entre las áreas de conservación prioritaria más valoradas en todo el mundo.
2. Aquí, evaluamos los efectos conjuntos tanto de factores bióticos (es decir, abundancia y riqueza de microorganismos y cobertura de vegetación y criptógamas) como abióticos (es decir, pH y aridez) sobre las fracciones de P lábil, de labilidad media y recalcitrante a lo largo de un amplio gradiente de aridez en la costa atlántica de la Península Ibérica.
3. El clima determinó la disponibilidad del P de labilidad media, recalcitrante y total, pero tuvo un efecto neto menor en el P lábil, el cual fue positivamente relacionado con la presencia de plantas, musgos y líquenes. El P de labilidad media fue positivamente y negativamente influenciado por la riqueza y la abundancia bacteriana del suelo, respectivamente.
4. Nuestros resultados sugieren que los microorganismos transfieren P de labilidad media a fracciones más lábiles. Al mismo tiempo, incrementos en la riqueza de bacterias asociadas a biofilms podrían estar involucrados en el engrosamiento de la fracción de P de labilidad media en nuestra secuencia climática.
5. Estas transferencias mediadas por bacterias le conferirían resistencia al P lábil bajo un escenario de cambio climático futuro y revelaría el importante papel de los microorganismos del suelo como moduladores del ciclo geoquímico del P.

**Palabras claves**: biofilms, secuencia climática, dunas costeras, cambio global, fósforo de labilidad media, modelo de transferencia microbiana, fracciones de fósforo.

## 1. Introduction

Phosphorus (P) and nitrogen (N) are traditionally considered the most limiting nutrients in terrestrial ecosystems, but the global increase of atmospheric N deposition is expected to intensify P limitation (Peñuelas et al., 2013; Yue et al., 2016). As a result, a growing attention has been paid to understand the P cycle as a regulator of key ecological processes (Feng et al., 2016; Hou, Chen, et al., 2018; Turner, Wells, & Condron, 2014) . However, the role of climate — including its indirect effect through biotic and abiotic drivers — on the availability of P remains largely unexplored and little understood. In the soil, P interacts with minerals, dead organic matter, microbes, and plants, and is regulated by climate, which makes particularly challenging to fully understand its cycle (Ruttenberg, 2003). The dynamics and bioavailability of soil inorganic and organic P forms are predominantly controlled by geochemical but also by biological processes. Soil P is associated to mineral fractions that are mostly unavailable for organisms on the short term (Shafqat, Shahid, Eqani, & Shah, 2016). Thus, depending on soil chemical conditions (e.g. pH), soluble phosphate can precipitate, forming insoluble minerals with Ca, Fe or Al, adsorbed by sesquioxides (Weng, Van Riemsdijk, & Hiemstra, 2012), or be incorporated into soil organic matter and other soil colloids (Lambers, Raven, Shaver, & Smith, 2008). Under biological control, the P is linked to plant production and to microbial immobilization and mineralization. Thus, vascular plants influence soil P directly (litterfall) and indirectly, since they are able to develop efficient P uptake mechanisms (e.g. mycorrhizal symbioses) (Belnap, 2011; Lajtha & Schlesinger, 1988). Cryptograms (mosses and lichens) along with soil microbes also have a key role in controlling soil P availability through secretion of organic acids, which solubilize bound P (Jones & Oburger, 2011), and respiration (excretion of $H^+$), which diminishes soil pH and releases P bound to carbonate (Belnap, 2011).

Both geochemical and biological controls on soil P cycling are ultimately dependent on climate (Belnap, 2011; Hou, Chen, et al., 2018) since it determines both geochemical weathering and biological activity (Chadwick, Kelly, Hotchkiss, & Vitousek, 2007). For instance, increases in temperature have been shown to increase occluded P by favoring geochemical processes such as P sorption on secondary minerals (Hou, Chen, et al., 2018),

and to reduce P availability due to the effect of drier conditions on biological activity (Belnap, 2011). Precipitation can influence P losses through chemical weathering of primary mineral P (Walker & Syers, 1976) followed by surface runoff (Sims, Simard, & Joern, 1998). Also, increases in aridity have important effects on P biogeochemistry, by inducing nutrient unbalances and changes in P pools (Delgado-Baquerizo et al., 2013; Feng et al., 2016; Jiao et al., 2016), which are also affected by variations in soil organic matter (OM), microbial communities or pH (Hou, Wen, et al., 2018; Jones & Oburger, 2011; Shen et al., 2011). For example, microbial abundance and activity are strongly affected by soil pH (Aciego Pietri & Brookes, 2008; Hou, Chen, et al., 2018; Maestre et al., 2015), which at the same time drives organic P mineralization and solubilization of fixed P (Shen et al., 2011).

Current climatic models forecast widespread aridity increases in terrestrial ecosystems worldwide (Huang, Yu, Guan, Wang, & Guo, 2016). Climate change is also likely have major impacts on the P cycle (Belnap, 2011; Hou, Chen, et al., 2018), but we do not know how changes in aridity will influence the availability of different soil P fractions with different lability, particularly in coastal dune areas. Dunes rank among the most valued priority conservation areas worldwide because of their high biodiversity (Acosta, Carranza, & Izzi, 2009; Lomba, Alves, & Honrado, 2008; Maltez-Mouro, Maestre, & Freitas, 2010; Mikkonen & Moilanen, 2012). Moreover, they have a critical role in mitigating the impacts of extreme weather events (Bellard, Bertelsmeier, Leadley, Thuiller, & Courchamp, 2012; Jentsch et al., 2011), such as hurricanes, which are likely to become more frequent in the future because of climate change (Diffenbaugh et al., 2017; Harley et al., 2006; Knutson et al., 2010). Understanding how climate change affects soil P pools in coastal dunes is essential to better understand its impacts on these key ecosystems. Doing so is also important to inform on potential conservation strategies, as primary production in dune areas is frequently limited by P (Kachi & Hirose, 1983), and vegetation plays a critical role stabilizing the dune substrate and protecting inland areas from extreme events (Silva, Martínez, Odériz, Mendoza, & Feagin, 2016).

Herein, we studied a climosequence composed of 24 areas in the Atlantic-Mediterranean coastline of the Iberian Peninsula to evaluate both the effects of geochemical and biological drivers on different soil P pools varying in their stability (i.e. labile, medium-lability, recalcitrant and total P). We hypothesized that: i) increases in aridity will be directly linked to lower soil P pools (Belnap, 2011; Feng et al., 2016; Hou, Chen, et al., 2018), which, in turn, will be positively affected by increases in, organic matter content, microbial diversity and abundance and changes in soil pH (Hou, Wen, et al., 2018; Jones & Oburger, 2011; Shen

et al., 2011); and that ii) labile P fractions will be mainly affected by biological processes, while more stable P fractions will be mainly controlled by geochemical processes, which are strongly influenced by climate (Condron, Turner, & Cade-Menun, 2005; Cross & Schlesinger, 2001).

## 2. Material and methods

### *2.1.Study area and climatic data*

We carried out this study in 24 coastal dune ecosystems located along a ~1500 km, northwest-to-southeast climosequence across the Iberian Peninsula (Table S1, Figure S1). Their climate ranged from Mediterranean with oceanic influences to Mediterranean dry (Köppen-Geiger Classification; Kottek *et al.*, 2006). Mean annual precipitation (MAP) and temperature (MAT), annual potential evapotranspiration (PET) and aridity index (UNEP, 1992) for each sampling site were extracted from WorldCLIM 2.0 (Fick & Hijmans, 2017) and Global Aridity and PET (CGIAR-CSI) datasets (Trabucco & Zommer, 2019) respectively, using R version 3.5.1. (rgdal and raster packages; R Core Team, 2018, Vienna, Austria). Climate data was averaged for the reference period 1970-2000. MAP and MAT ranged from 1441 mm/year and ~13.8ºC, respectively, in the north-west, to 225 mm/year and ~18ºC, respectively, in the south-east. Aridity was determined based on the UNEP Aridity Index (AI), following the equation:

$$Aridity = 1 - (AI), where AI = \frac{MAP}{PET} \quad (1)$$

Our climosequence covered a wide aridity gradient, as it ranged from -0.28 to 0.86 from north-west to south-east (see AI in Figure S1). Aridity was highly correlated with both MAP and MAT along the gradient surveyed (Figure S2).

Soils were classified as Arenosols derived from aeolian sands (IUSS Working Group WRB, 2014). Stabilized dunes (i.e. the last stage of dune systems development, which allows colonization of perennial plant species) along the climosequence were well conserved and the sandy substrate fixed by scrubs, shrubs and arboreal vegetation. Dominant perennial plant species were mainly *Ammophila arenaria* (L) Link, *Helichrysum picardii* (Boiss. & Reuter), *Crucianella marítima* (L.), among others (see Table S1 for a full list of species and climate characteristics of each plot).

The features of the studied sites, which show large differences in climate and photosynthetic cover (from 20% to 100%) but share the same soil type, minimize the usual soil type-related confounding factors in observational studies carried out over large areas, which facilitates the study of the effects of climate. We identified three microsites with different prevalence along the climosequence: plant (areas under the canopy of vascular plants), cryptogams (areas under mosses and lichens) and bare soil (areas without any visible photosynthetic cover). For some of the analyses, the plots along the aridity gradient were divided in three groups based on the local heterogeneity of microsites. The first group ("Humid sites"), included those plots (n=9) which were located in the north part of the gradient (Figure S1), and was characterized by the absence of bare soil areas, so the entire plot surface was covered either by plants or cryptogams (mostly mosses). The second group ("Mesic sites") was defined by those plots where the three microsites were clearly identified and covered a significant part of the plot. These plots (n=4) were located in the mid part of the aridity gradient. Finally, the third group ("Dry sites") included those plots (n=11) having only plant and bare soil microsites, which were located in the southern and eastern part of the gradient.

*2.2.Field survey and soil samples processing*

We sampled our study sites in July 2016. For each site, we established a 30 × 30 m plot parallel to the coastline. We used the line-point intercept method for estimating both biotic cover and plant community composition in each plot (Brun & Box, 1963). In total, we sampled 4 transects of 25 m of length in each plot. Data of species was noted every 20 cm along each transect. As most of the sites had a patched vegetation cover intermixed with bare soil and cryptogamic patches, we carried out a stratified soil sampling in the three main microsites described above (plants, cryptogams and bare soil). For each microsite, we collected five, randomly located soil samples from the top 10 cm of the soil profile using a 10 × 10 × 10 cm square sampler. We pooled soil samples of each microsite to make composite samples. Visible roots and stones were carefully removed from all soil samples before sieving (2 mm mesh). Soil samples were collected in the dry season
to reduce bias between aridity gradient sites as a result of seasonal changes in the soil variables studied (Delgado-Baquerizo et al., 2016), air dried in the lab for one month and stored in polyethylene bags until analyses. We also kept a set of field-moist subsamples at -20ºC for microbiological analysis. Soil pH was measured with a pH meter, in a 1:2.5

(mass:volume, soil:water) suspension. Soil organic matter content was determined by loss on ignition at 450 °C for 4 h (Nelson & Sommers, 1996).

*2.3.Phosphorus fractionation*

We quantified both labile and more stable P fractions using a modified sequential extraction method by Tiessen & Moir, 1993, which is based on the Hedley fractionation technique (Hedley, Stewart, & Chauhan, 1982) (Figure S3). This method estimates different P fractions of decreasing bioavailability. Inorganic P ($P_i$) extracted with ion exchange resins (Resin $P_i$) represents the most bioavailable P pool, which is absorbed on surfaces of soil crystalline compounds. Bicarbonate-extractable P is weakly absorbed by soil colloids, and is still available for plant uptake. Both $P_i$ and organic P ($P_o$), extracted with NaOH, are strongly chemisorbed by Fe-Al components within the soil, and are considered medium term plant-available P. Finally, the procedure ends with the extraction of the most stable forms of P, HCl-extractable Pi, which is typically associated to Ca in soils, and residual P, which represents the pool from the primary mineral such as apatite (Hedley et al., 1982; Tiessen, Stewart, & Cole, 1984).

In short, 0.5 g of soil samples were placed in 50 mL polyethylene centrifuge tubes together with 30 mL of demineralized water and two 4 × 2 cm anion-exchange membranes (AMI-7001S, Membranes International Inc., New Jersey). After tubes were shaken, resins were removed and placed in clean 50 mL tubes adding 0.7M NaCl to extract $PO_4^-$. Then, soil samples were sequentially extracted with 30 mL aliquots of 0.5M $NaHCO_3$ (adjusted to pH 8.5), 0.1M NaOH, 1M HCl, and 0.5M $H_2SO_4$ after 550 °C of soil combustion (Figure S3). For each extraction, tubes were shaken for 16 hours and then centrifuged at 900 g for 30 minutes (Guppy, Menzies, Moody, Compton, & Blamey, 2000). The concentration of $PO_4^{3-}$-P in the supernatant was used to estimate $P_i$ associated to each P fraction. We estimated $P_o$ fractions by subtracting $P_i$ from the total P obtained after digesting the $P_o$ into $P_i$ in the 0.5M $NaHCO_3$, and 0.1M NaOH extracts. We used an alkaline digestion with 0.148M $K_2S_2O_8$ and 3M NaOH for the $NaHCO_3$ extract ($NaHCO3\text{-}P_t$), and an acid digestion with $(NH_4)_2S_2O_8$ and 0.9M $H_2SO_4$ for the NaOH extract ($NaOH\text{-}P_t$). Both digestions were made in the autoclave at 121 ℃ for 1 h and 1h 30 min, respectively (Tiessen & Moir, 2006). For the determination of residual P, soil samples were heated in a furnace at 550 ºC for 1h. Then, the burned soil residue was extracted with 5 mL of 0.5M $H_2SO_4$, shaken for 1h, filtered and the $PO_4^{3-}$ concentration measured in this extract (Chen et al., 2015). We used the Malachite Green

Method (Fernández *et al.*, 1985; modified from Hess & Derr, 1975) to estimate $PO_4^{3-}$-P concentration in the extracts. Malachite green has been found to be the most sensitive basic dye for phosphate determination (Itaya & Ui, 1966; Rahutomo, Kovar, & Thompson, 2019). The pH of the extracts was adjusted to neutral pH to reach a correct colour development of samples as necessary. The absorbance of samples was measured at 655 nm wavelength by triplicate in a microplate reader (Jupiter, Asys Hitech GmbH).

The different P fractions were grouped in categories according to temporary P availability. We estimated labile P ($P_L$, i.e. short-term bioavailable P) pool as the sum of Resin $P_i$ and $NaHCO_3$ $P_t$, whereas medium-lability P ($P_{ML}$) pool was defined as the sum of NaOH $P_t$ and HCl $P_i$. Recalcitrant P ($P_R$) pool was the residual P fraction derived from primary minerals as apatite and long-term bioavailable P (Cross & Schlesinger, 1995; Hedley et al., 1982; Tiessen et al., 1984; Walker & Syers, 1976). Finally, Total P ($P_T$) was calculated as the sum of all the extracted P fractions.

*2.4.Bacterial and fungal abundance*

Soil total metagenomic DNA was extracted from 0.5 g of frozen soil using the PowerSoil DNA isolation kit (MOBIO Laboratories, Inc. Carlsbad, CA, USA) following the manufacturer's protocol, except for modifications in the lysis step [we used a tissue homogeniser (Precellys 24-dual, Bertin technologies, Montigny-le Bretonneux, France) at 4500 rpm for 45 s, twice]. The abundance of total soil fungi and bacteria was determined with real-time quantitative PCR (q-PCR) using 96-well plates on an ABI 7300 Real-Time PCR (Applied Biosystems, Foster City, CA. USA). Total fungal 18S and bacterial 16S r-RNA genes abundances were quantified in duplicate and then pooled using primer pairs ITS1F/5.8s and Eub338/Eub518, respectively (Evans & Wallenstein, 2012; Maestre et al., 2015). The reaction mixture contained 2 µl of DNA template (4 ng/µl), 5 µl of PowerUpTM SYBR Green Master Mix (2x) (Applied Biosystems, Foster City, CA, USA), 0.3 µl of each primer (0.4 mM) and 0.4 µl of BSA (0.4 mg/ml) in a total volume of 10 µl.

*2.5.Bacterial and fungal richness – high throughput sequencing and bioinformatics*

DNA extractions were frozen and delivered to the Next Generation Genome Sequencing Facility of the University of Western Sydney (Australia) for amplicon sequencing using Illumina Miseq platform. Richness of soil bacteria and fungi were derived from the amplicon sequencing on the bacterial 16S rRNA gene and fungal Internal transcribed spacer (ITS) sequence, respectively. Primer pair 341F/805R was used for bacterial 16S rDNA v3-v4

region (Herlemann et al., 2011); primer pair FITS7/ITS4 was used for fungal ITS sequence (Ihrmark et al., 2012). Raw reads were quality-controlled and merged using USEARCH (Edgar, 2010), and merged reads with expected error lower than 0.5 were filtered. Error correction on amplicons were performed using UNOISE3 (Edgar, 2016), with 100% identity for Operational Taxonomic Unit determination (i.e. zOTU). Bacterial and fungal richness were calculated from the zOTU table at a resampling depth of 14187 and 18924 reads per sample, respectively.

*2.6.Statistical analysis*

Regression analyses were carried out to test linear and polynomial relationships between aridity and the concentrations of the different P pools. The appropriate model selection was based on AIC values. Previously to calculate plot-level concentration of each P pool, we calculated the weighted average of the three microsites taking into account the area of the plot covered by each of them (Durán et al., 2018; Maestre et al., 2012). For each site (*humid, mesic and dry*), we performed linear mixed model with microsite as fixed factor and plot as random factor to explore the influence of microsite on the different P pools, as well as post-hoc tests, lsmeans package (Lenth, 2016), to compare the different microsites in each type of plots. Data were transformed to logarithm when necessary to normalize their distribution.

We used structural equation modelling (SEM; Grace, 2006) to evaluate the direct and indirect effects of aridity, microsite (bare soil/photosynthetic cover) and soil properties (pH, organic matter content, bacterial and fungal abundance and richness) on the concentration of the different P pools (see Figure S4 for our priori model). Based on the the chi-squared test ($\chi^2$; the model has a good fit when $\chi^2$/df is $\leq 2$, and P is $> 0.05$), the root-mean-square error of approximation (RMSEA; the model has a good fit when RMSEA is indistinguishable from zero, and P is $> 0.05$), as well as the Bollen-Stine bootstrap tests (Hooper, Coughlan, & Mullen, 2008; Schermelleh-Engel, Moosbrugger, & Müller, 2003) we tested the overall goodness of fit of our SEM. After verifying the adequate fit of our model, we interpreted the path coefficients of the model and their associated *P*-values. A path coefficient is analogous to the partial correlation coefficient or regression weight, and describes the strength and sign of the relationships between two variables (Grace, 2006). As our data were not always normally distributed we used bootstrap tests to assess whether the probability that a path coefficient differs from zero (Kline, 2011; Schermelleh-Engel et al., 2003). We calculated the standardized total effects of all drivers on the selected P fractions. The net influence that one

variable had upon another was calculated by summing all direct and indirect pathways (effects) between two variables.

Regression analyses and mixed-effect models, nlme package (Pinheiro, Bates, DebRoy, Sarkar, & R Core Team, 2019) were conducted with the software R, version 3.5.1. (R Core Team, 2018, Vienna, Austria). All SEM analyses were conducted using the software AMOS 24.0 (IBM SPSS, Chicago, IL, USA).

## 3. Results

Across the gradient, most of the total P (ca. 72%) was found in the medium-lability P pool (Table 1). The remaining total P was distributed in similar amounts between labile and recalcitrant P. The labile P pool comprised ca. 1/3 of resin-P and 2/3 of $NaHCO_3$-P. The majority (ca. 80%) of the medium-lability P was composed by the HCl-$P_i$ fraction, whereas similar amounts of organic and inorganic P were found in the less abundant NaOH fraction.

Soil concentrations of medium-lability P ($P_{ML}$), recalcitrant P ($P_R$) and total P ($P_T$) were negatively related to aridity (F ($P_{ML}$)= 8.17; F ($P_T$)= 8.7; F ($P_R$)= 8.69, respectively; df= 22 and $p<0.01$ for all cases) (Figure 1b, 1c and 1d; see Table S2 and S3 for F-and *p*-values of the relationships among climatic variables and all P pools/fractions, respectively). Conversely, labile P ($P_L$) was not significantly related to aridity (Figure 1; see Figure S5 for regressions between MAT, MAP and all P pools).

Our SEM explained 73% of the variation in soil total P (Figure 2a). Soil total P was significantly and negatively influenced by aridity and bacterial abundance, but positively by pH, organic matter (OM) and bacterial richness. We did not find significant relationships among fungal abundance or richness and any variable included in our SEMs, so both were discarded from the SEMs analysis. We also found negative indirect effects of aridity (through reductions in bacterial richness), positive indirect effects of pH (through increases in bacterial richness), and negative indirect effects of OM (through increases in bacterial abundance) on soil total P. The standardized total effects (sum of direct and indirect effects) indicated that aridity and pH were the most important predictors of soil $P_T$, with a negative and positive influence, respectively. In contrast to soil $P_T$, our SEM only explained 37% of the soil $P_L$ variation (Figure 2b). Soil $P_L$ was positively and significantly related to soil OM, suggesting an important biologic origin of this pool. We did not find a significant direct effect of aridity on soil $P_L$. The standardized total effects showed that the main drivers of soil $P_L$ were OM and pH, both with a positive influence. Our SEM was able to explain 68% of the variation in

the $P_{ML}$ (Figure 2c). Soil pH, OM and bacterial richness showed a positive direct effect on the mid-term available P, while bacterial abundance and aridity showed a negative direct influence. Our results also showed negative indirect effects of aridity (through reductions on bacterial richness), pH (through increases in bacterial richness), and OM (through its positive effect on bacterial abundance) on this P pool. The negative direct effect of microbial abundance on soil medium-lability P unveil a microbial transfer of medium-lability to labile P as shown in Figure 3. The most important predictors of $P_{ML}$ were aridity and pH, with a negative and positive influence, respectively. Finally, our SEM was only able to explain 47 % of the variation in soil $P_R$, and we only found a positive direct effect of aridity on this P pool (Figure 2d).

In dry sites, the effect of microsite was significant for $P_L$ and $P_T$, which were higher under the canopy of vascular plants than in bare ground soils ($F = 6.31$, $p<0.05$; $F = 5.26$, $p<0.05$, respectively; Figure 4a and 4d), suggesting that the short-term availability of P is biologically driven. The differences in $P_L$ were due to the higher amounts of resin P found under vegetation ($F=10.45$, $p<0.01$), whereas higher NaOH $P_i$ concentration ($F= 8.57$, $p<0.05$) at this microsite contributed to the higher Pt as compared with bare ground soils. In humid sites, we detected significant higher amounts of resin P under vascular plants than under cryptogams (mosses) ($F= 12.68$, $p<0.001$), reflecting the dominance of mineralization over immobilization by microorganisms under vascular plants (but not under mosses). We did not find significant differences among microsites in mesic sites for any P fraction (See Table 1 for means and standard errors of the different P pools/fractions concentrations).

## 4. Discussion

Our study provides new insights on soil homeostasis of the most available P pool along an aridity gradient, giving support to the hypothesis of the decoupling of N and P cycles with increasing aridity described by Delgado-Baquerizo et al. (2013). Further, it may also help to explain the more general balance of the N and P cycles predicted under global change scenarios (Peñuelas et al., 2013). Delgado-Baquerizo et al. (2013) suggested that a higher mechanical weathering rate may be behind the relative higher P availability compared to C and N observed under high aridity conditions in global drylands. Our results suggest an additional mechanism mediated by microorganisms (bacterial abundance) that would transfer P from medium-lability pool to more labile one (Figure 3) contributing to the thickening of this bioavailable soil P pool. This mechanism would confer resistance to the P labile pool to

changes in aridity, and may be a complementary mechanism explaining the relatively high P availability respect to N with increasing aridity (Delgado-Baquerizo et al., 2013). More generally, this resistance of the labile P pool based on the multiple biological and geochemical interactions may determine P availability under scenarios of increasing N deposition.

We hypothesized that all P pools should be influenced by aridity. However, significant negative slopes were only found between aridity and medium-lability P, recalcitrant P, and total P indicating lower weathering rates as aridity increases. Higher precipitation should enhance greater chemical weathering rates throughout its effects on both soil properties and biotic communities (Dixon, Chadwick, & Vitousek, 2016; White & Blum, 1995), resulting in the accumulation of the stable forms of P in the soil profile until leaching does not overcome weathering rates. Hou et al. (2018), using a global dataset of 96 published articles including a wide range of precipitation (31-6000 mm/yr), found that some P fractions (available P, primary mineral P and soil total P) were negatively affected by mean annual precipitation as an effect of the leaching of the weathered minerals with high precipitation (Hou, Chen, et al., 2018). In the precipitation range studied here (225-1441 mm/yr), leaching intensity of weathered minerals should be less relevant (Austin & Vitousek, 1998). Thus, the balance of P as a result of geochemical processes (i.e. weathering and/or dust deposition rates vs. leaching and/or erosion rates) may be negative in more humid biomes (e.g. tropical systems), but positive in dryland ecosystems (Turner, Wells, Andersen, & Condron, 2018; Vitousek & Chadwick, 2013). Indeed, changes in P pools along a climosequence induced by the effect of precipitation on geochemical and physical processes were also found by Feng et al. (2016). These authors described that total P decreased with increasing aridity, but this tendency reverted in sites with aridity values > 0.8 due to P accumulation.

Interestingly, we expected that climate controls on stable P were mirrored by labile P pool, but the lack of any significant relationship between labile P and aridity suggested, as indicated above, a high resistance for this pool, with important implications for the ongoing environmental global change. Thus, if available P stays stable with aridity, the unbalance in the C, N and P bioavailability will be driven by relative increases in C and N availability (Delgado-Baquerizo et al., 2013; Menge, Hedin, & Pacala, 2012), which may exacerbate the P demand by organisms (Peñuelas et al., 2013; Vitousek, Porder, Houlton, & Chadwick, 2010). In any case, our results suggest that, because of the rapid turnover rate of labile P pool (Shafqat et al., 2016), available P would be more dependent on mechanisms such as P uptake

by plant roots, the rapid sorption of P in occluded mineral forms, and microbially related processes (mineralization, immobilization and solubilization) than on long-term macroclimatic effects (Austin & Vitousek, 1998; Belnap, 2011; Castenholz & Garcia-pichel, 2012; Verrecchia et al., 1995). Indeed, both the significance change of plant community cover and our explicit consideration of the different microsites present along the climosequence (i.e. plant- and cryptogam-covered areas as well as bare soil areas without any visible photosynthetic cover) add support to the idea that inorganic anions, secreted by plant roots or derived from OM mineralization, could compete for adsorption sites of calcium carbonate minerals increasing the availability of P under vegetation and also highlight the contribution of litter to soil P content (Cross & Schlesinger, 2001; Shen et al., 2011). Thus, we could highlight the important role of the spatial distribution of the vegetation cover in both labile and total P.

In turn, our results show that changes in soil pH affected medium-lability P, underlining the influence of pH on P availability (Shen et al., 2011). Alkaline soils, characterized by a major content of calcium cations, promotes the precipitation of inorganic phosphorus as calcite or di-calcium phosphates (Belnap, 2011). Therefore, the high content of calcium carbonates ($CaCO_3$) from seashells on coastal soils could explain the highest concentrations of calcium phosphates (Cross & Schlesinger, 2001; Staunton & Leprince, 1996), which represents approximately 80% of medium-lability P in our dune climosequence.

We found a strong association between bacteria and medium-lability P, with bacterial abundance and bacterial richness having opposed effects. While the capacity of bacteria to solubilize P from minerals is well known (Shrivastava, Srivastava, & D'Souza, 2018) and may explain a bacterial abundance-mediated transfer from medium-lability P to labile P, the possibility that bacteria (and its richness) could increase this (mostly) mineral pool (adsorption of P in soil surfaces mediated by bacteria) is, to the best of our knowledge, largely unknown for terrestrial soils. However, microbial-mediated P adsorption has been described in marsh and wetland soils (e.g. Rejmánková & Komárková, 2000; Scinto & Reddy, 2003) and has been recognized as one of the most important mechanisms involved in the withdrawal of available P in sewage treatment plants (De-Bashan & Bashan, 2004; Lu, Yang, Shabbir, & Wu, 2014). The mechanism involves the adsorption of large amounts of P in the extracellular polymeric substances (EPS) secreted by biofilms. We believe that this mechanism may also explain the positive effects of bacteria richness on medium-lability P because: first, increasing evidence shows that biofilms are the predominant mode of life for

soil microorganisms (Flemming & Wuertz, 2019; Gutiérrez Castorena et al., 2016; Kuzyakov & Blagodatskaya, 2015); second, soil biofilms are directly related with bacterial diversity (Wu et al., 2019); and finally, significant amounts of EPS are found in aerobic soils (Wang et al., 2019). Thus, beyond the well-known microbial control of the biological cycle of soil P, we suggest that the geochemical cycle may also be, at least partially, under biological control.

Our findings provide novel insights on how biotic and abiotic factors affect different P pools in stabilized dune ecosystems. The results obtained emphasize the negative effect that climate change can have on the total reserves and on the less labile fractions of P in coastal dune soils. Likewise, they highlight the higher resistance of the most labile P fractions, which provides a better understanding of the imbalance of P availability regarding their N and C counterparts with increasing aridity. Interestingly, they also uncover a mechanism not described so far about bacterial-mediated P transfers between different P fractions, which directly attributes an important modulator role of soil microorganisms on the geochemical P cycle in terrestrial ecosystems.

**References**


Aciego Pietri, J. C., & Brookes, P. C. (2008). Relationships between soil pH and microbial properties in a UK arable soil. *Soil Biology & Biochemistry*, *40*, 1856–1861. https://doi.org/10.1016/j.soilbio.2008.03.020

Acosta, A., Carranza, M. L., & Izzi, C. F. (2009). Combining land cover mapping of coastal dunes with vegetation analysis. *Applied Vegetation Science*, *8*(2), 133–138. https://doi.org/10.1111/j.1654-109X.2005.tb00638.x

Arnold, E. (1992). United Nations Environment Programme. In *World atlas of desertification* (p. 287). https://doi.org/10.1002/ldr.3400030407

Austin, A. T., & Vitousek, P. (1998). Nutrient dynamics on a rainfall gradient in Hawai'i. *Oecologia*, *113*, 519–529.

Baxter, S. (2015). World Reference Base for Soil Resources 2014. In *World Soil Resources Reports No. 106*. https://doi.org/10.1017/S0014479706394902

Bellard, C., Bertelsmeier, C., Leadley, P., Thuiller, W., & Courchamp, F. (2012). Impacts of climate chang on the future of biodiversity. *Ecology Letters*, *15*, 365–377. https://doi.org/10.1111/j.1461-0248.2011.01736

Belnap, J. (2011). Biological Phosphorus Cycling in Dryland Regions. In E. Bünemann, A. Oberson, & E. Frossard (Eds.), *Phosphorus in Action* (pp. 371–406). https://doi.org/10.1007/978-3-642-15271-9

Brun, J. M., & Box, W. T. (1963). Comparison of line intercepts and random point frames for sampling desert shrub vegetation. *Journal of Range Management*, *16*(1), 21–25. https://doi.org/10.2307/3895032

Castenholz, R. W., & Garcia-pichel, F. (2012). Cyanobacterial responses to UV radiation. In *Ecology of Cyanobacteria II: Their Diversity in Space and Time* (pp. 481–499). https://doi.org/10.1007/978-94-007-3855-3_19

Chadwick, O. A., Kelly, E. F., Hotchkiss, S. C., & Vitousek, P. M. (2007). Precontact vegetation and soil nutrient status in the shadow of Kohala Volcano , Hawaii. *Geomorphology*, *89*, 70–83. https://doi.org/10.1016/j.geomorph.2006.07.023

Chen, C. R., Hou, E. Q., Condron, L. M., Bacon, G., Esfandbod, M., Olley, J., & Turner, B. L. (2015). Geoderma Soil phosphorus fractionation and nutrient dynamics along the Cooloola coastal dune chronosequence , southern Queensland , Australia. *Geoderma*. https://doi.org/10.1016/j.geoderma.2015.04.027

Condron, L. M., Turner, B. L., & Cade-Menun, B. J. (2005). Chemistry and Dynamics of Soil Organic Phosphorus. In *Agronomy* (pp. 87–121). https://doi.org/10.2134/agronmonogr46.c4

Cross, A. F., & Schlesinger, W. H. (1995). A literature review and evaluation of the. Hedley fractionation: Applications to the biogeochemical cycle of soil phosphorus in natural ecosystems. *Geoderma*, *64*(3–4), 197–214. https://doi.org/10.1016/0016-7061(94)00023-4

Cross, A. F., & Schlesinger, W. H. (2001). Biological and geochemical controls on phosphorus fractions in semiarid soils. *Biogeochemistry*, *52*(2), 155–172. https://doi.org/10.1023/A:1006437504494

De-Bashan, L. E., & Bashan, Y. (2004). Recent advances in removing phosphorus from wastewater and its future use as fertilizer (1997-2003). *Water Research*, *38*(19), 4222–4246. https://doi.org/10.1016/j.watres.2004.07.014

Delgado-Baquerizo, M., Maestre, F. T., Eldridge, D. J., Bowker, M. A., Ochoa, V., Gozalo,

B., … Singh, B. K. (2016). Biocrust-forming mosses mitigate the negative impacts of increasing aridity on ecosystem multifunctionality in drylands. *New Phytologist*, *209*(4), 1540–1552. https://doi.org/10.1111/nph.13688

Delgado-Baquerizo, M., Maestre, F. T., Gallardo, A., Bowker, M. A., Wallenstein, M. D., Quero, J. L., … Zaady, E. (2013). Decoupling of soil nutrient cycles as a function of aridity in global drylands. *Nature*, *502*(7473), 672–676. https://doi.org/10.1038/nature12670

Diffenbaugh, N. S., Singh, D., Mankin, J. S., Horton, D. E., Swain, D. L., Touma, D., … Rajaratnam, B. (2017). Quantifying the influence of global warming on unprecedented extreme climate events. *Proceedings of the National Academy of Sciences*, *114*(19), 4881–4886. https://doi.org/10.1073/pnas.1618082114

Dixon, J. L., Chadwick, O. A., & Vitousek, P. M. (2016). Climate-driven thresholds for chemical weathering in postglacial soils of New Zealand. *Journal of Geophysical Research: Earth Surface*, *121*(9), 1619–1634. https://doi.org/10.1002/2016JF003864

Durán, J., Delgado-Baquerizo, M., Dougill, A. J., Guuroh, R. T., Linstädter, A., Thomas, A. D., & Maestre, F. T. (2018). Temperature and aridity regulate spatial variability of soil multifunctionality in drylands across the globe. *Ecology*, *99*(5), 1184–1193. https://doi.org/10.1002/ecy.2199

Edgar, R. C. (2010). Search and clustering orders of magnitude faster than BLAST. *Bioinformatics*, *26*(19), 2460–2461. https://doi.org/10.1093/bioinformatics/btq461

Edgar, R. C. (2016). UNOISE2: improved error-correction for Illumina 16S and ITS amplicon sequencing. *BioRxiv*, 081257. https://doi.org/10.1101/081257

Evans, S. E., & Wallenstein, M. D. (2012). Soil microbial community response to drying and rewetting stress : does historical precipitation regime matter ? *Biogeochemistry*, *109*, 101–116. https://doi.org/10.1007/s10533-011-9638-3

Feng, J., Turner, B. L., Lü, X., Chen, Z., Wei, K., Tian, J., … Chen, L. (2016). Phosphorus transformations along a large-scale climosequence in arid and semiarid grasslands of northern China. *Global Biogeochemical Cycles*, *30*, 1264–1275. https://doi.org/10.1002/2015GB005331

Fernández, J. A., Niell, F. X., & Lucena, J. (1985). A rapid and sensitive automated

determination of phosphate in natural waters. *Limnology and Oceanography*, *30*(1), 227–230. https://doi.org/10.4319/lo.1985.30.1.0227

Fick, S. E., & Hijmans, R. J. (2017). WorldClim 2: new 1-km spatial resolution climate surfaces for global land areas. *International Journal of Climatology*, *37*(12), 4302–4315. https://doi.org/10.1002/joc.5086

Flemming, H. C., & Wuertz, S. (2019). Bacteria and archaea on Earth and their abundance in biofilms. *Nature Reviews Microbiology*, *17*(4), 247–260. https://doi.org/10.1038/s41579-019-0158-9

Grace, J. B. (2006). *Structural equation modeling and natural systems*. Cambridge University Press.

Guppy, C. N., Menzies, N. W., Moody, P. W., Compton, B. L., & Blamey, F. P. C. (2000). A simplified, sequential, phosphorus fractionation method. *Communications in Soil Science and Plant Analysis*, *31*(11–14), 1981–1991. https://doi.org/10.1080/00103620009370556

Gutiérrez Castorena, E. V., Gutiérrez-Castorena, M. del C., González Vargas, T., Cajuste Bontemps, L., Delgadillo Martínez, J., Suástegui Méndez, E., & Ortiz Solorio, C. A. (2016). Micromapping of microbial hotspots and biofilms from different crops using digital image mosaics of soil thin sections. *Geoderma*, *279*, 11–21. https://doi.org/10.1016/j.geoderma.2016.05.017

Harley, C. D. G., Hughes, A. R., Kristin, M., Miner, B. G., Sorte, C. J. B., & Carol, S. (2006). The impacts of climate change in coastal marine systems. *Ecology Letters*, *9*, 228–241. https://doi.org/10.1111/j.1461-0248.2005.00871.x

Hedley, M. J., Stewart, J. W. B., & Chauhan, B. S. (1982). Changes in Inorganic and Organic Soil Phosphorus Fractions Induced by Cultivation Practices and by Laboratory Incubations. *Soil Science Society of America Journal*, *46*(5), 970–976.

Herlemann, D. P. R., Labrenz, M., Jürgens, K., Bertilsson, S., Waniek, J. J., & Andersson, A. F. (2011). Transitions in bacterial communities along the 2000 km salinity gradient of the Baltic Sea. *ISME Journal*, *5*(10), 1571–1579. https://doi.org/10.1038/ismej.2011.41

Hess, H. H., & Derr, J. E. (1975). Assay of inorganic and organic phosphorus in the 0.1-5 nanomole range. *Analytical Biochemistry*, *63*(2), 607–613. https://doi.org/10.1016/0003-

2697(75)90388-7

Hooper, D., Coughlan, J., & Mullen, M. (2008). Structural equation modelling: Guidelines for determining model fit. *Electronic Journal of Business Research Methods*, *6*(1), 53–60. https://doi.org/10.1037/1082-989X.12.1.58

Hou, E., Chen, C., Luo, Y., Zhou, G., Kuang, Y., Zhang, Y., … Wen, D. (2018). Effects of climate on soil phosphorus cycle and availability in natural terrestrial ecosystems. *Global Change Biology*, *24*(8), 3344–3356. https://doi.org/10.1111/gcb.14093

Hou, E., Wen, D., Kuang, Y., Cong, J., Chen, C., He, X., … Zhang, Y. (2018). Soil pH predominantly controls the forms of organic phosphorus in topsoils under natural broadleaved forests along a 2500 km latitudinal gradient. *Geoderma*, *315*(April), 65–74. https://doi.org/10.1016/j.geoderma.2017.11.041

Huang, J., Yu, H., Guan, X., Wang, G., & Guo, R. (2016). Accelerated dryland expansion under climate change. *Nature Climate Change*, *6*(2), 166–171. https://doi.org/10.1038/nclimate2837

Ihrmark, K., Bödeker, I. T. M., Cruz-Martinez, K., Friberg, H., Kubartova, A., Schenck, J., … Lindahl, B. D. (2012). New primers to amplify the fungal ITS2 region - evaluation by 454-sequencing of artificial and natural communities. *FEMS Microbiology Ecology*, *82*(3), 666–677. https://doi.org/10.1111/j.1574-6941.2012.01437.x

Itaya, K., & Ui, M. (1966). A new micromethod for the colorimetric determination of inorganic phosphate. *Clinica Chimica Acta*, *14*, 361–366.

Jentsch, A., Kreyling, J., Elmer, M., Gellesch, E., Glaser, B., Grant, K., … Beierkuhnlein, C. (2011). Climate extremes initiate ecosystem-regulating functions while maintaining productivity. *Journal of Ecology*, *99*(3), 689–702. https://doi.org/10.1111/j.1365-2745.2011.01817.x

Jiao, F., Shi, X. R., Han, F. P., & Yuan, Z. Y. (2016). Increasing aridity, temperature and soil pH induce soil C-N-P imbalance in grasslands. *Scientific Reports*, *6,19601*, 1–9. https://doi.org/10.1038/srep19601

Jones, D. L., & Oburger, E. (2011). Solubilization of Phosphorus by Soil Microorganisms. In *Phosphorus in Action* (Vol. 26, pp. 169–198). https://doi.org/10.1007/978-3-642-15271-9_7

Kachi, N., & Hirose, T. (1983). Limiting Nutrients for Plant Growth in Coastal Sand Dune Soils. *The Journal of Ecology*, *71*(3), 937. https://doi.org/10.2307/2259603

Kline, R. B. (2011). Principles and Practice of Structural Equation Modeling, 3rd edn Guilford Press. *New York*.

Knutson, T. R., McBride, J. L., Chan, J., Emanuel, K., Holland, G., Landsea, C., … Sugi, M. (2010). Tropical cyclones and climate change. *Nature Geoscience*, *3*, 157–163. https://doi.org/10.1038/ngeo779

Kottek, M., Grieser, J., Beck, C., Rudolf, B., & Rubel, F. (2006). World Map of the Köppen-Geiger climate classification updated. *Meteorologische Zeitschrift*, *15*(3), 259–263. https://doi.org/10.1127/0941-2948/2006/0130

Kuzyakov, Y., & Blagodatskaya, E. (2015, April 1). Microbial hotspots and hot moments in soil: Concept & review. *Soil Biology and Biochemistry*, Vol. 83, pp. 184–199. https://doi.org/10.1016/j.soilbio.2015.01.025

Lajtha, K., & Schlesinger, W. H. (1988). The biogeochemistry of phosphorus cycling and phosphorus availability along a desert soil chronosequence. *Ecological Society of America*, *69*(1), 24–39.

Lambers, H., Raven, J. A., Shaver, G. R., & Smith, S. E. (2008). Plant nutrient-acquisition strategies change with soil age. *Trends in Ecology and Evolution*, *23*(2), 95–103. https://doi.org/10.1016/j.tree.2007.10.008

Lenth, R. V. (2016). Least-Squares Means: The R Package lsmeans. *Journal of Statistical Software*, *69*(1). https://doi.org/10.18637/jss.v069.i01

Lomba, A., Alves, P., & Honrado, J. (2008). Endemic Sand Dune Vegetation of the Northwest Iberian Peninsula: Diversity, Dynamics, and Significance for Bioindication and Monitoring of Coastal Landscapes. *Journal of Coastal Research*, *2*, 113–121. https://doi.org/10.2112/05-0610.1

Lu, H., Yang, L., Shabbir, S., & Wu, Y. (2014). The adsorption process during inorganic phosphorus removal by cultured periphyton. *Environmental Science and Pollution Research*, *21*(14), 8782–8791. https://doi.org/10.1007/s11356-014-2813-z

Maestre, F. T., Delgado-Baquerizo, M., Jeffries, T. C., Eldridge, D. J., Ochoa, V., Gozalo, B., … Singh, B. K. (2015). Increasing aridity reduces soil microbial diversity and

abundance in global drylands. *Proceedings of the National Academy of Sciences*, *112*, 15684–15689. https://doi.org/10.1073/pnas.1516684112

Maestre, F. T., Quero, J. L., Gotelli, N. J., Escudero, A., Ochoa, V., Delgado-Baquerizo, M., … Zaady, E. (2012). Plant species richness and ecosystem multifunctionality in global drylands. *Science*, *335*(6065), 214–218. https://doi.org/10.1126/science.1215442

Maltez-Mouro, S., Maestre, F. T., & Freitas, H. (2010). Co-occurrence patterns and abiotic stress in sand-dune communities: Their relationship varies with spatial scale and the stress estimator. *Acta Oecologica*, *36*(1), 80–84. https://doi.org/10.1016/j.actao.2009.10.003

Menge, D. N. L., Hedin, L. O., & Pacala, S. W. (2012). Nitrogen and phosphorus limitation over long-term ecosystem development in terrestrial ecosystems. *PLoS ONE*, *7*(8). https://doi.org/10.1371/journal.pone.0042045

Mikkonen, N., & Moilanen, A. (2012). Identification of top priority areas and management landscapes from a national Natura 2000 network. *Environmental Science and Policy*, *27*, 11–20. https://doi.org/10.1016/j.envsci.2012.10.022

Nelson, D. W., & Sommers, L. E. (1996). Total Carbon , Organic Carbon , and Organic Matter. In *Methods of Soil Analysis. Part 3. Chemical Methods, (ed Sparks DL), American Society of Agronomy-Soil Science Society of America, Madison, WI.* (pp. 539–594).

Peñuelas, J., Poulter, B., Sardans, J., Ciais, P., van der Velde, M., Bopp, L., … Janssens, I. a. (2013). Human-induced nitrogen–phosphorus imbalances alter natural and managed ecosystems across the globe. *Nature Communications*, *4*(1), 2934. https://doi.org/10.1038/ncomms3934

Pinheiro, J., Bates, D., DebRoy, S., Sarkar, D., & R Core Team, 2019. (2019). Nlme: Linear and Nonlinear Mixed Effects Models.

Rahutomo, S., Kovar, J. L., & Thompson, M. L. (2019). Malachite Green Method for Determining Phosphorus Concentration in Diverse Matrices. *Communications in Soil Science and Plant Analysis*, *50*(14), 1743–1752. https://doi.org/10.1080/00103624.2019.1635140

Rejmánková, E., & Komárková, J. (2000). A function of cyanobacterial mats in phosphorus-

limited tropical wetlands. In *Hydrobiologia* (Vol. 431).

Ruttenberg, K. C. (2003). The Global Phosphorus Cycle. In *Treatise on Geochemistry* (pp. 585–643).

Schermelleh-Engel, K., Moosbrugger, H., & Müller, H. (2003). Evaluating the fit of structural equation models: Tests of significance and descriptive goodness-of-fit measures. *Methods of Psychological Research Online*, *8*(2), 23–74. https://doi.org/10.1002/0470010940

Scinto, L. J., & Reddy, K. R. (2003). Biotic and abiotic uptake of phosphorus by periphyton in a subtropical freshwater wetland. *Aquatic Botany*, *77*(3), 203–222. https://doi.org/10.1016/S0304-3770(03)00106-2

Shafqat, M., Shahid, S., Eqani, S., & Shah, S. (2016). Soil phosphorus fractionation as a tool for monitoring dust phosphorus signature underneath a Blue Pine ( Pinus wallichiana ) canopy in a Temperate Forest. *Forest Systems*, *25*(3). https://doi.org/10.5424/fs/2016253-09337

Shen, J., Yuan, L., Zhang, J., Li, H., Bai, Z., Chen, X., … Zhang, F. (2011). Phosphorus Dynamics: From Soil to Plant. *Plant Physiology*, *156*(3), 997–1005. https://doi.org/10.1104/pp.111.175232

Shrivastava, M., Srivastava, P. C., & D'Souza, S. F. (2018). Phosphate-solubilizing microbes: Diversity and phosphates solubilization mechanism. In *Role of Rhizospheric Microbes in Soil: Volume 2: Nutrient Management and Crop Improvement* (pp. 137–165). https://doi.org/10.1007/978-981-13-0044-8_5

Silva, R., Martínez, M. L., Odériz, I., Mendoza, E., & Feagin, R. A. (2016). Response of vegetated dune-beach systems to storm conditions. *Coastal Engineering*, *109*, 53–62. https://doi.org/10.1016/j.coastaleng.2015.12.007

Sims, J. T., Simard, R. R., & Joern, B. C. (1998). Phosphorus Loss in Agricultural Drainage: Historical Perspective and Current Research. *Journal of Environment Quality*, *27*(2), 277. https://doi.org/10.2134/jeq1998.00472425002700020006x

Staunton, S., & Leprince, F. (1996). Effect of pH and some organic anions on the solubility of soil phosphate : implications for P bioavailability. *European Journal of Soil Science*, (47), 231–239.

Tiessen, H., & Moir, J. . (2006). Characterization of Available P by Sequential Extraction. In *Soil Sampling and Methods of Analysis* (p. 14). https://doi.org/10.1201/9781420005271.ch25

Tiessen, H., Stewart, J. W. B., & Cole, C. V. (1984). Pathways of Phosphorus Transformations in Soils of Differing Pedogenesis. *Soil Science Society of America Journal*, *48*, 853–858.

Title, P. O., & Bemmels, J. B. (2018). ENVIREM: an expanded set of bioclimatic and topographic variables increases flexibility and improves performance of ecological niche modeling. *Ecography*, *41*(2), 291–307. https://doi.org/10.1111/ecog.02880

Turner, B. L., Wells, A., Andersen, K. M., & Condron, L. M. (2018). Consequences of the physical nature of the parent material for pedogenesis, nutrient availability, and succession in temperate rainforests. *Plant and Soil*, *423*(1–2), 533–548. https://doi.org/10.1007/s11104-017-3514-4

Turner, B. L., Wells, A., & Condron, L. M. (2014). Soil organic phosphorus transformations along a coastal dune chronosequence under New Zealand temperate rain forest. *Biogeochemistry*, *121*(3), 595–611. https://doi.org/10.1007/s10533-014-0025-8

Verrecchia, E., Yair, A., Kidron, G. J., Verrecchia, K., Campus, R., Jerusalem, I.-, & Campus, G. R. (1995). Physical properties of the psammophile cryptogamic crust and their consequences to the water regime of sandy soils, north-western Neveg Desert, Israel. *Journal of Arid Environments*, *29*, 427–437.

Vitousek, P. M., & Chadwick, O. A. (2013). Pedogenic Thresholds and Soil Process Domains in Basalt-Derived Soils. *Ecosystems*, *16*(8), 1379–1395. https://doi.org/10.1007/s10021-013-9690-z

Vitousek, P. M., Porder, S., Houlton, B. Z., & Chadwick, O. A. (2010). Terrestrial phosphorus limitation: Mechanisms, implications, and nitrogen-phosphorus interactions. *Ecological Applications*, *20*(1), 5–15. https://doi.org/10.1890/08-0127.1

Walker, T. W., & Syers, J. K. (1976). The fate of phosphorus during pedogenesis. *Geoderma*, *15*(1), 1–19. https://doi.org/10.1016/0016-7061(76)90066-5

Wang, S., Redmile-Gordon, M., Mortimer, M., Cai, P., Wu, Y., Peacock, C. L., … Huang, Q. (2019). Extraction of extracellular polymeric substances (EPS) from red soils (Ultisols).

*Soil Biology and Biochemistry*, *135*, 283–285. https://doi.org/10.1016/j.soilbio.2019.05.014

Weng, L., Van Riemsdijk, W. H., & Hiemstra, T. (2012). Factors Controlling Phosphate Interaction with Iron Oxides. *Journal of Environment Quality*, *41*(3), 628. https://doi.org/10.2134/jeq2011.0250

White, A. F., & Blum, A. E. (1995). Effects of climate on chemical weathering in watersheds. *Geochimica et Cosmochimica Acta*, *59*(9), 1729–1747.

Wu, Y., Cai, P., Jing, X., Niu, X., Ji, D., Ashry, N. M., … Huang, Q. (2019). Soil biofilm formation enhances microbial community diversity and metabolic activity. *Environment International*, *132*, 105116. https://doi.org/10.1016/j.envint.2019.105116

Yue, K., Peng, Y., Peng, C., Yang, W., Peng, X., & Wu, F. (2016). Stimulation of terrestrial ecosystem carbon storage by nitrogen addition : a meta-analysis. *Science Reports*, *6*, 1–10. https://doi.org/10.1038/srep19895

**Tables and figures**

**Table 1.** Concentration (mean + SE) of fractions/pools P (mg/kg) along the climosequence studied. Weighted (taking into account the proportion of each microsite within the plot, N=25) and microsite-level values are presented. P fractions grouped by lability: $P_L$ (labile P), $P_{ML}$ (medium-lability P), $P_R$ (recalcitrant P) and $P_T$ (total P). Average percentage for P fractions grouped by lability are in brackets.

| P fractions | Weighted plot | Microsites | | | | | | |
|---|---|---|---|---|---|---|---|---|
| | | Humid sites (N = 9) | | | Mesic sites (N = 4) | | Dry sites (N = 11) | |
| | | Cryptogam | Vegetation | Bare soil | Cryptogam | Vegetation | Bare soil | Vegetation |
| Resin P | 4.6 (0.4) | 4.4 (0.5) | 5.4 (0.5) | 4.6 (0.5) | 2.4 (0.5) | 3.6 (1.0) | 3.9 (0.6) | 6.2 (1.0) |
| $NaHCO_3$ $P_i$ | 8.5 (0.9) | 9.6 (1.5) | 11 (1.6) | 5.1 (1.4) | 5.4 (1.6) | 5.1 (1.7) | 8.1 (1.9) | 8.0 (1.4) |
| $NaHCO_3$ $P_o$ | 4.9 (0.5) | 4.5 (1.2) | 6.0 (2.2) | 7.4 (1.5) | 6.9 (1.2) | 5.7 (1.5) | 4.0 (0.7) | 7.0 (1.5) |
| $NaHCO_3$ $P_t$ | 13.3 (0.9) | 14.2 (1.7) | 17.0 (2.1) | 12.5 (0.7) | 12.2 (1.4) | 10.9 (0.9) | 11.2 (1.3) | 15.0 (2.1) |
| NaOH $P_i$ | 6.1 (0.8) | 6.1 (1.6) | 6.8 (1.6) | 9.4 (1.1) | 7.8 (1.4) | 9.0 (1.9) | 3.6 (0.7) | 5.6 (0.9) |
| NaOH $P_o$ | 5.9 (0.6) | 7.0 (0.9) | 6.4 (0.6) | 9.7 (1.9) | 9.0 (2.2) | 7.6 (1.9) | 3.8 (0.9) | 4.8 (0.8) |
| NaOH $P_t$ | 12.0 (1.2) | 13. (2.3) | 13.1 (2.1) | 19.0 (1.4) | 16.9 (1.9) | 16.6 (1.4) | 7.4 (1.1) | 10.3 (1.2) |
| HCl $P_i$ | 84.6 (8.8) | 119.6 (10.0) | 116.4 (9.7) | 76.7 (9.4) | 67.9 (6.8) | 91.3 (16.3) | 57.6 (12.9) | 57.4 (12.6) |
| Residual P | 18.8 (1.8) | 23.4 (3.8) | 22.4 (3.0) | 20.3 (4.4) | 20.9 (3.5) | 20.1 (3.8) | 15.6 (1.3) | 15.0 (1.3) |
| **P fractions grouped by lability** | | | | | | | | |
| $P_L$(16%) | 17.9 (1.2) | 18.6 (2.2) | 22.3 (2.3) | 17.0 (1.0) | 14.7 (1.8) | 14.5 (1.4) | 15.1 (14.6) | 21.2 (2.9) |
| $P_{ML}$ (68%) | 96.5 (9.0) | 132.6 (9.6) | 129.4 (9.4) | 95.7 (8.9) | 84.7 (4.9) | 107.9 (15.9) | 65.0 (1.6) | 67.7 (12.5) |
| $P_R$ (16%) | 18.8 (1.8) | 23.4 (3.8) | 22.4 (3.0) | 20.3 (4.4) | 20.9 (3.5) | 20.1 (3.8) | 13.6 (12.9) | 15.0(1.3) |
| $P_T$ | 133.2 (10.6) | 174.6 (10.8) | 174.2 (12.2) | 133.1 (13.6) | 120.3 (6.6) | 142.45 (18.9) | 93.6 (14.6) | 103.5 (14.8) |

**Figure captions**

**Figure 1.** Relationship between aridity and labile, medium-lability, recalcitrant and total P (mg/kg soil). Black circles, solid lines and asterisk represent each sampling point (n=24), the fitted linear regressions and significance of $P < 0.05$, respectively.

**Figure 2.** Effects of aridity, bacterial abundance (BA), bacterial richness (BR), organic matter (OM) and pH on total (a), labile (b), medium-lability (c) and recalcitrant (d) soil P pools. Right panels show the total (direct plus indirect) effects derived from the structural equation modelling. Numbers on arrows and width of lines are indicative of the effect size of the relationship. Continuous and dashed arrows indicate significant and not significant relationships, respectively. Positive and negative relationships are represented in red and blue lines, respectively. Significance levels are as follows: ˙, $P < 0.10$; *, $P < 0.05$; **, $P < 0.01$.

**Figure 3.** Microbial transfer model between medium-lability P and labile P mediated by bacterial abundance and bacterial richness. Bacterial abundance would transfer P from medium-lability to more labile pool and bacterial richness would have opposed effects increasing mostly mineral P pool through adsorption of P.

**Figure 4**. Differences between microsites (vascular vegetation and cryptogams and bare ground areas) in labile, medium-lability, recalcitrant and total P in humid (n=9), mesic (n=4) and dry (n=11) sites. Differences between microsites ($p < 0.05$) are indicated by different lowercase letters.

**Figure 1**

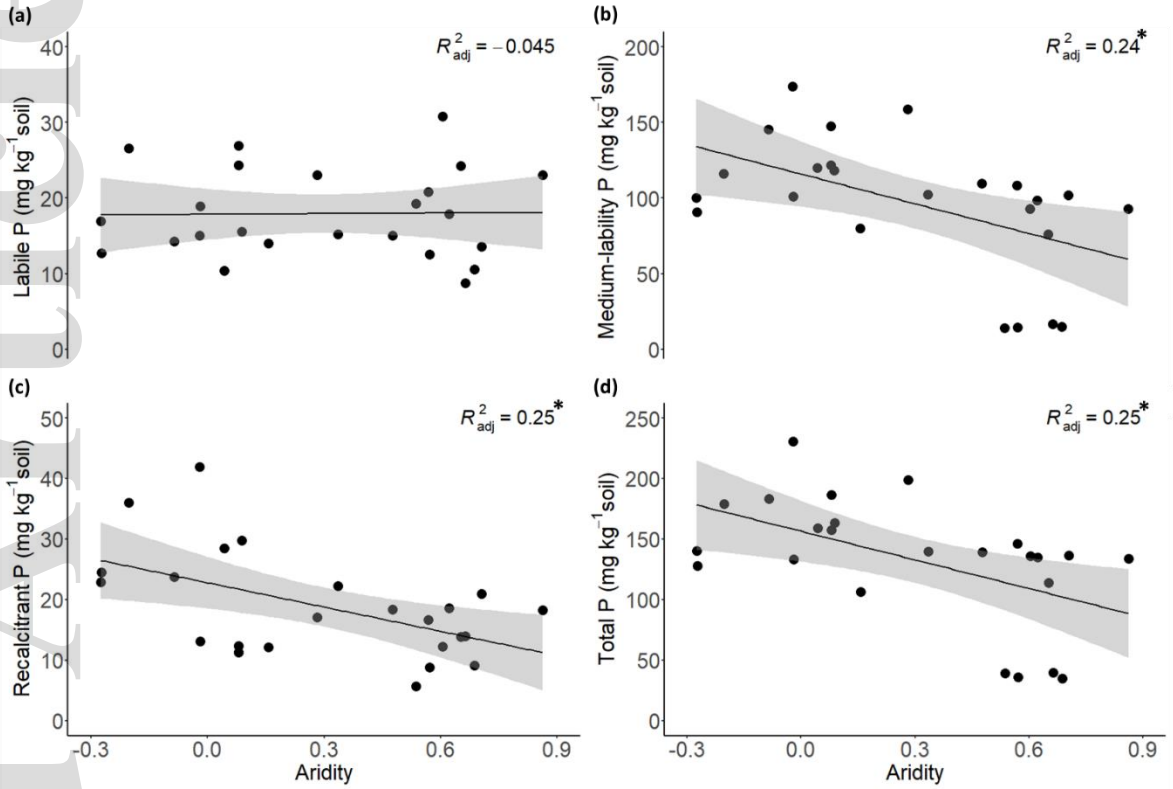

**Figure 2**

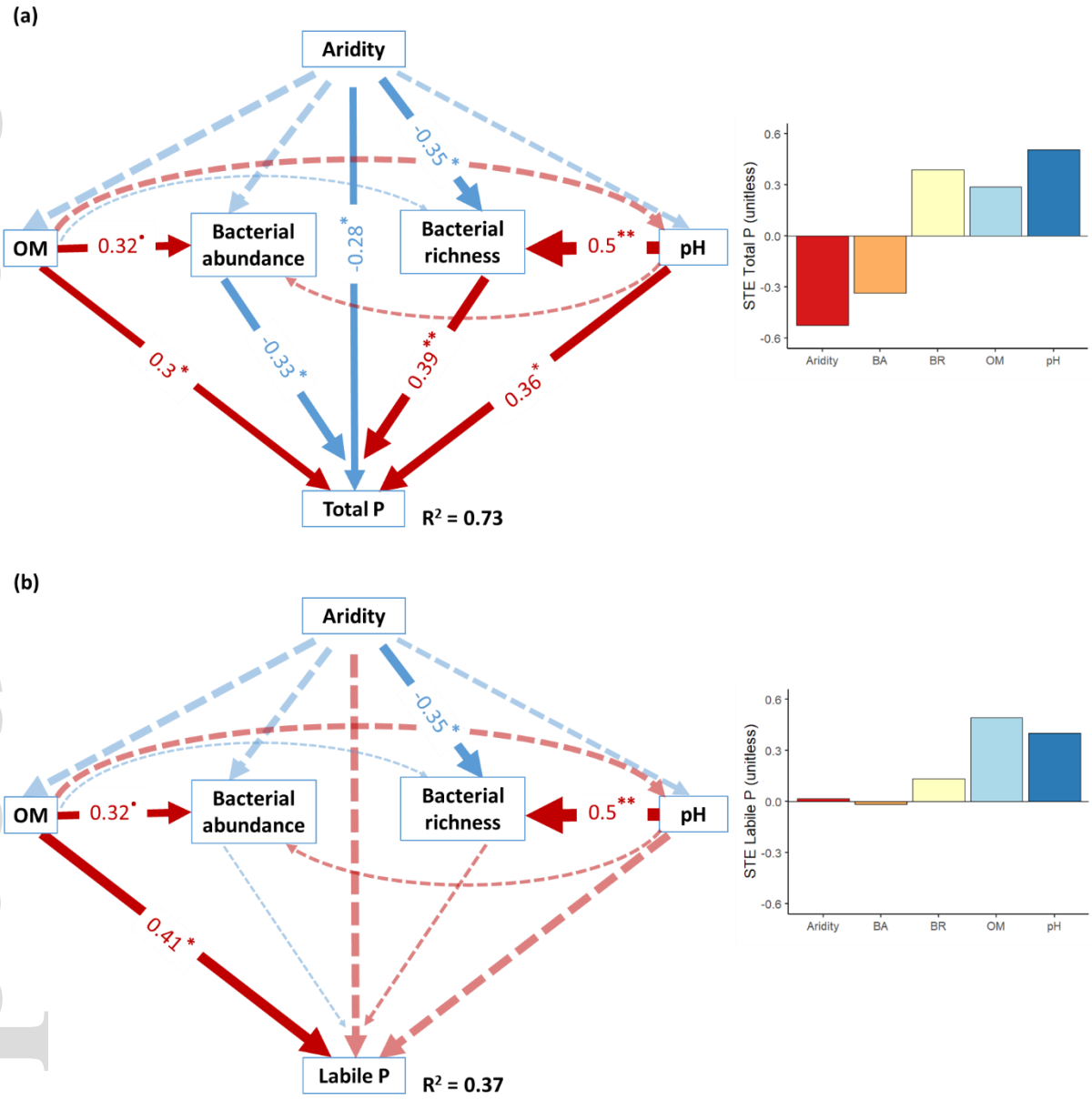

(c)

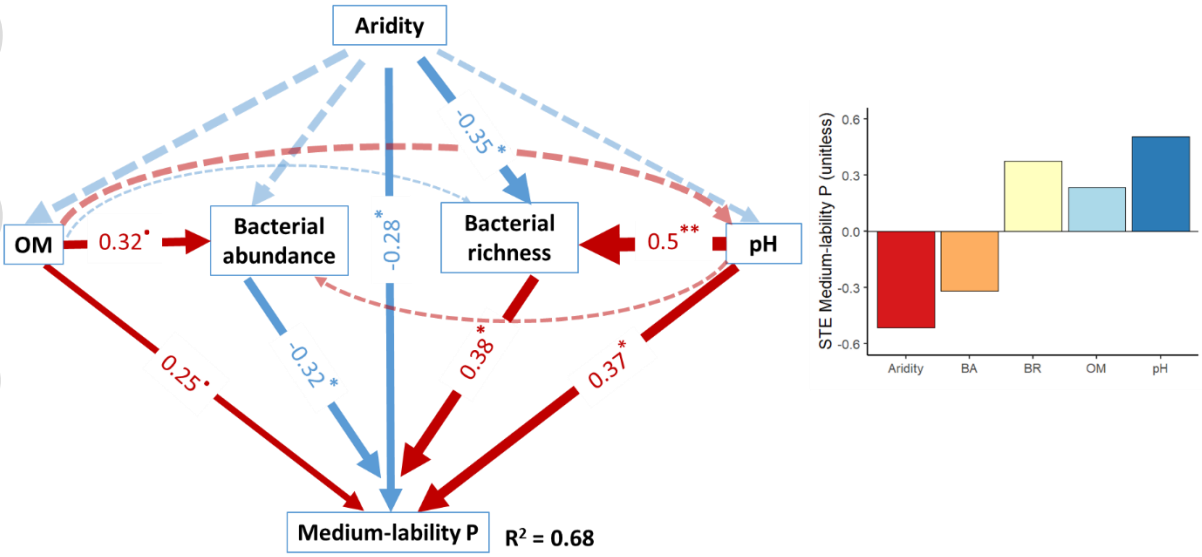


(d)

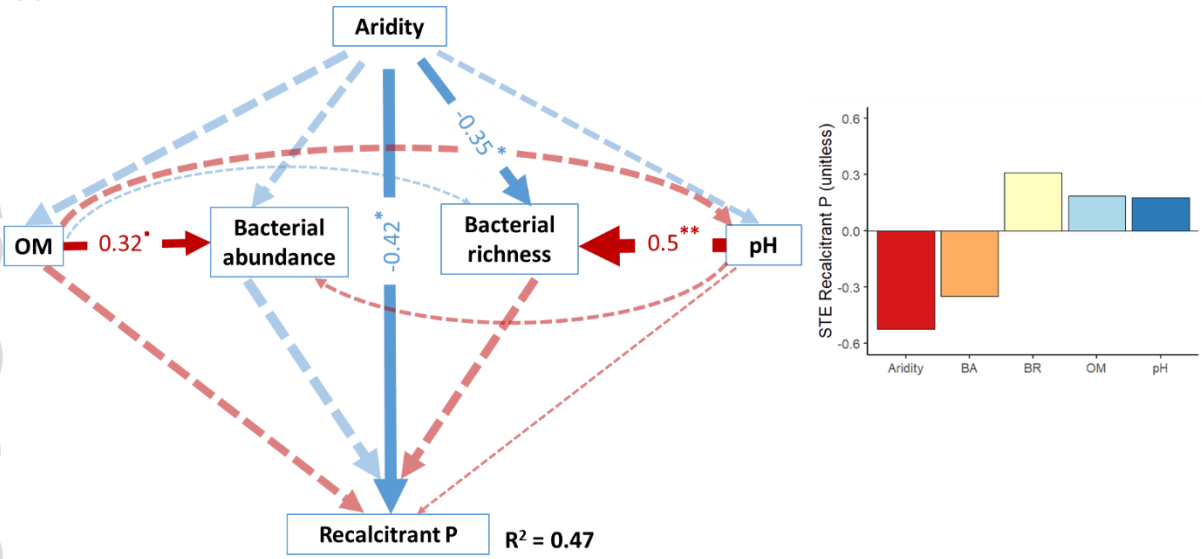

**Figure 3**

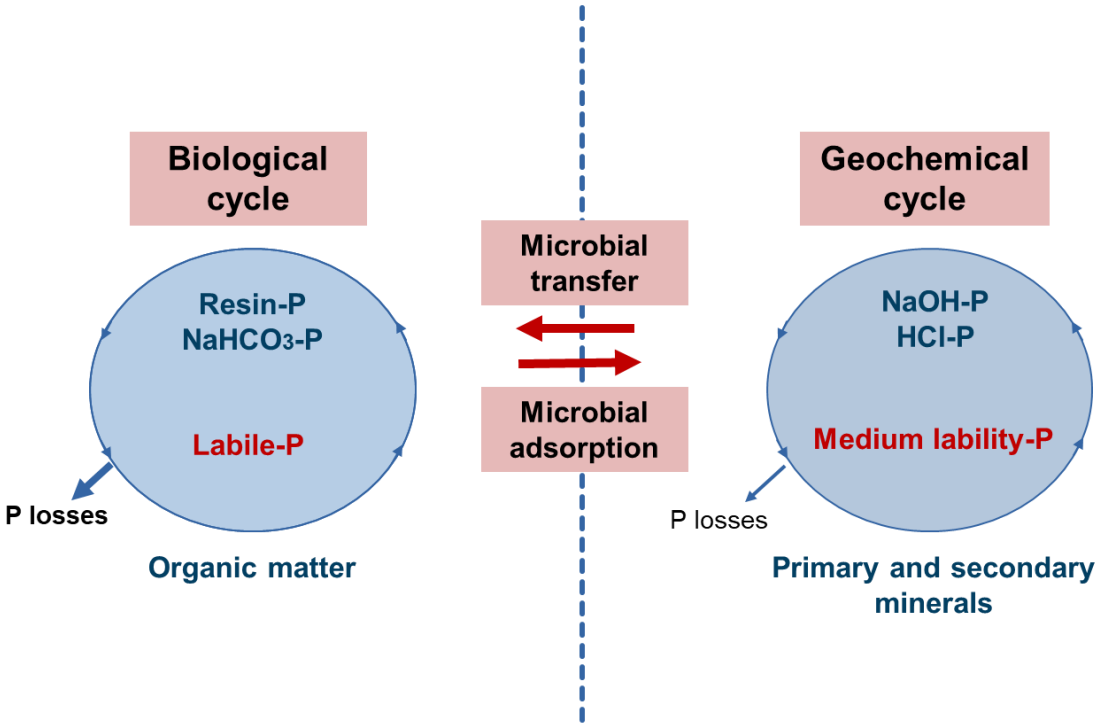

**Figure 4**

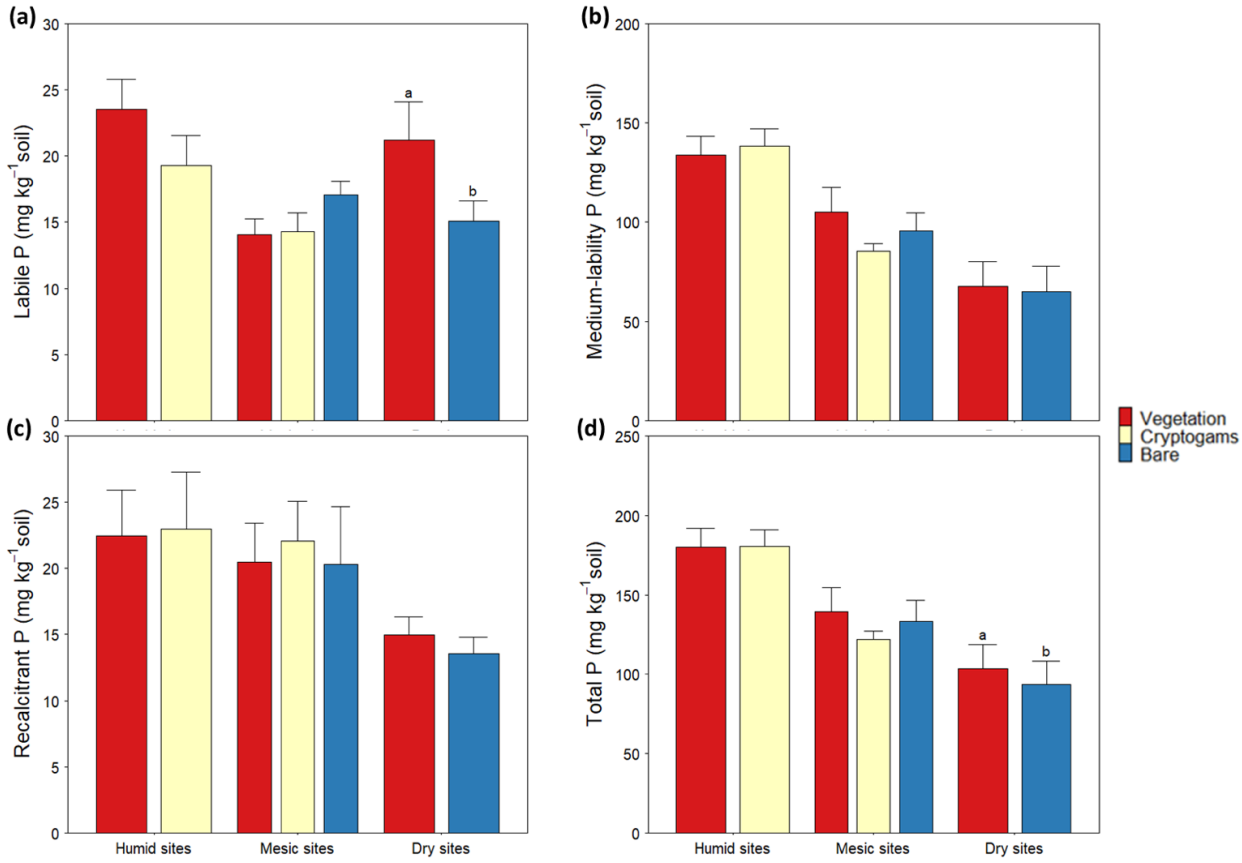
(a)
Labile P (mg kg$^{-1}$soil)
30
25
20
15
10
5
0
a
b
(b)
Medium-lability P (mg kg$^{-1}$soil)
200
150
100
50
0
(c)
Recalcitrant P (mg kg$^{-1}$soil)
30
25
20
15
10
5
0
Humid sites
Mesic sites
Dry sites
(d)
Total P (mg kg$^{-1}$soil)
250
200
150
100
50
0
a
b
Humid sites
Mesic sites
Dry sites
Vegetation
Cryptogams
Bare